Amino Acids (2010) 38:613–622
DOI 10.1007/s00726-009-0420-y

ORIGINAL ARTICLE

Proteomic analysis of livers from a transgenic mouse line with activated polyamine catabolism

Marc Cerrada-Gimenez · Jukka Häyrinen · Sisko Juutinen · Tuula Reponen · Juhani Jänne · Leena Alhonen

Received: 20 July 2009 / Accepted: 8 September 2009 / Published online: 10 December 2009

Abstract We have generated a transgenic mouse line that over expresses the rate-controlling enzyme of the polyamine catabolism, spermidine/spermine N^1-acetyltransferase, under the control of a heavy metal inducible promoter. This line is characterized by a notable increase in SSAT activity in liver, pancreas and kidneys and a moderate increase in the rest of the tissues. SSAT induction results in an enhanced polyamine catabolism manifested as a depletion of spermidine and spermine and an overaccumulation of putrescine in all tissues. To study how the activation of polyamine catabolism affects other metabolic pathways, protein expression pattern of the livers of transgenic animals was analyzed by two-dimensional polyacrylamide gel electrophoresis and mass spectrometry. A total of 23 proteins were shown to be differentially expressed in the transgenic from the wild-type animals. Many of the identified proteins showed expression patterns associated with polyamine catabolism activation. However, the expression pattern of other proteins, such as repression of GST pi and selenium-binding protein 2 and 60 kDa heat-shock protein, could be explained by the overexpression of peroxisome proliferator-activated receptor γ co-activator 1α in response to depleted ATP pools. The activation of the latter proteins is thought to lead to the improved insulin sensitivity seen in the MT-SSAT animals.

M. Cerrada-Gimenez (✉) · S. Juutinen · T. Reponen · J. Jänne · L. Alhonen
Department of Biotechnology and Molecular Medicine, A.I. Virtanen Institute for Molecular Sciences, University of Kuopio, P.O.Box 1627, 70211 Kuopio, Finland
e-mail: Marc.CerradaGimenez@uef.fi

J. Häyrinen
Department of Biosciences/Biochemistry, University of Kuopio, P.O.Box 1627, 70211 Kuopio, Finland

Keywords Polyamines · Proteomics · SSAT · Liver · Transgenic mouse

Abbreviations

2D-PAGE	Two-dimensional polyacrylamide gel electrophoresis
AdoHcy	*S*-Adenosylhomocysteine
AdoMet	*S*-Adenosyl-L-methionine
IPG	Immobilized pH gradient
MS	Mass spectrometry
PPAR	Peroxisome proliferator-activated receptor
PGC-1α	Peroxisome proliferator-activated receptor γ co-activator 1α
SSAT	Spermidine/spermine N^1-acetyltransferase

Introduction

Polyamines are naturally occurring polycations found in all living organisms. Although they have been shown to be involved in many different cellular functions, their exact biological role remains still elusive. Polyamines are involved in each one of the steps of the molecular biology's central dogma, from DNA replication and transcription to RNA translation (Jänne et al. 2004). Among them, the triamine spermidine has a particular role of being the sole precursor for the unusual amino acid hypusine, an integral part of the eukaryotic translation initiation factor 5a (eIF5A) which is believed to be responsible for the synthesis of the first peptide bond during protein synthesis (Park et al. 1997). Polyamines also interact with and regulate membrane bound enzymes, such as transglutaminases, *N*-methyl-D-aspartate receptors, and inwardly rectifying K^+ channels (Wallace et al. 2003). Moreover,

elevated polyamine levels may induce abnormal growth, while too low levels may halt the cell cycle (Järvinen et al. 2006).

A large number of transgenic animal models, chemically synthesized analogs and metabolic inhibitors have been generated for the study of the polyamine metabolism (Jänne et al. 2004, 2005; Wallace and Fraser 2004). Among the mice lines, we have produced two transgenic mouse lines overexpressing the rate-controlling enzyme of the polyamine catabolism, spermidine/spermine N^1-acetyltransferase (SSAT) (EC 2.3.1.57). One of the lines carries the SSAT gene under the control of its endogenous promoter (SSAT), while the second line carries the SSAT gene under the control of the mouse heavy metal inducible promoter metallothionein I (MT-SSAT). Moreover, as a counterpart to these SSAT overexpressing lines, a knockout (SSATKo) line has been generated, as well. The transgenic SSAT overexpressing lines are characterized by ubiquitously increased SSAT activity, but especially in liver and pancreas. The increased SSAT activity affects the tissue polyamine pools, reducing spermidine and spermine and increasing putrescine levels (Suppola et al. 1999).

Recently, we have shown that the SSAT transgenic animals exhibit enhanced insulin sensitivity (Pirinen et al. 2007), whereas the SSATKo line becomes insulin resistant upon aging (Niiranen et al. 2006). The improved insulin sensitivity seen in the SSAT overexpressing mouse line is apparently related to the elevated expression of the peroxisome proliferator-activated receptor γ co-activator 1α (PGC-1α) (Pirinen et al. 2007).

We performed a proteomics analysis of the MT-SSAT transgenic livers to obtain more detailed information on how modifications of the polyamine flux affect related metabolic pathways. These analyses showed that the activation of polyamine catabolism affects the expression of a large number of proteins as well as pools of key liver metabolites, directly or indirectly related to polyamine metabolism. The proteomics results indicated that an acute activation of polyamine catabolism was linked to the increased hepatic PGC-1α expression. However, because elevated hepatic PGC-1α has been shown as a hallmark of diabetes (Koo et al. 2004), we further investigated plasma glucose and insulin levels in MT-SSAT transgenic mice. Interestingly, the results indicated hypoglycemia and hypoinsulinemia suggesting that this phenotype could be explained by elevated PGC-1α levels also in muscle and white adipose tissue (WAT), as seen in SSAT transgenic mouse line (Pirinen et al. 2007).

Materials and methods

Generation of transgenic mice

The generation of MT-SSAT transgenic mouse line used in this study has been described earlier (Suppola et al. 1999). Non-transgenic litter mates served as controls for the transgenic mice. The mice were housed on 12 h light/dark cycle and were fed ad libitum a regular laboratory chow diet. The animal experiments were approved by the Institutional Animal Care and Use Committee of the University of Kuopio and the Provincial Government.

Two-dimensional polyacrylamide gel electrophoresis (2D-PAGE)

Sample preparation

Three 4-month-old males per genotype, transgenic and non-transgenic were killed by CO_2 inhalation. The animals were perfused with icecold phosphate-buffered saline, and the whole liver was removed. Livers were further homogenized in a buffer containing 25 mM Tris pH 7.4, 0.1 mM EDTA, 1 mM DTT, and complete protease inhibitor cocktail (Roche, Penzberg, Germany). The protein preparations were stored at −70°C until further analyzed. The protein amount of each sample was measured using the Bradford protein assay (Bio-Rad, Hercules, CA, USA).

Methodology

The 2D-PAGE methodology has been outlined elsewhere (Görg et al. 2000). Briefly, the first dimension isoelectric focusing (IEF) was performed using 18 cm 3–10 immobilized pH gradient strips (IPG) (GE Healthcare, Uppsala, Sweden). The strips that contained 150 μg of total protein each were rehydrated for 12 h at 20°C with 350 μl of rehydration buffer. Samples were run in duplicate. The IEF was carried out in an IPGPhor II focusing unit (GE Healthcare), following the instructions supplied by the manufacturer. Prior to the second dimension, the IPG strips were equilibrated in a DTT buffer. The second dimension was run using a Protean II xi (Bio-Rad) using 12.5% acrylamide/bis acrylamide gels.

Gel visualization and software analysis

Following the run, the gels were fixed in a solution containing 30% methanol and 7.5% acetic acid for 30 min. After fixation, the gels were stained overnight with a sufficient volume of SYPRO Ruby stain (Bio-Rad). The gels were rinsed in a 10% methanol and 6% acetic acid solution for 30 min, and scanned in a Storm 860 imaging system (Molecular Dynamics Inc., Sunnyvale, CA, USA). The gel images were analyzed with the PDQuest v6.0 software (Bio-Rad). The spot intensities were normalized against the total intensity from all the valid spots from the gel, and the results were statistically analyzed by the Student's *t*-test

using the SPSS v14.0 software package (SPSS, Chicago, IL, USA).

In-gel digestion and protein identification by mass spectrometry

The differentially expressed spots were excised and in-gel digested using trypsin (Promega, Madison, WI, USA). Tryptic peptides were separated using Ultimate/Famos capillary LC system (LC Packings, Amsterdam, The Netherlands). The samples were trapped onto a PepMap 100 C18 precolumn, 300 µm × 5 mm (Dionex, Sunnyvale, CA, USA) in 0.1% formic acid (Sigma–Aldrich, Steinhelm, Germany) and 2% ACN (Sigma–Aldrich) at a flow rate of 30 µL/min.

After 3 min of loading and clean-up, the precolumn was automatically switched in-line with the PepMap 100 C18 analytical column (3 µm, 75 µm × 50 mm) (Dionex). The peptides were eluted using a linear ACN gradient starting from 95% of 0.1% formic acid, 5% ACN to 30% of 0.1% formic acid, 95% ACN in 35 min, and finally to 100% of 0.1% formic acid, 95% ACN in 40 min, at 200 nL/min. The total runtime was 80 min.

The LC was connected to mass spectrometer by a nano-ESI ion source (MDS Sciex, South San Francisco, CA, USA) using distally coated 15-µm PicoTip emitters (New Objective, MS Wil GmbH, Switzerland).

Mass spectra were recorded in positive mode on a QSTAR XL hybrid quadrupole TOF instrument (Applied Biosystems Foster City, CA, USA) using information-dependent acquisition (IDA) for obtaining MS/MS data for sequence tag approach (Mann and Wilm 1994). For each run, 1-s TOF MS survey scans were recorded for mass range *m/z* 400-2,000 followed by 4 s MS/MS scans of the two most intense 2^+ and 3^+ charged ions (mass range *m/z* 30-1,600). Known trypsin autolytic fragment ions *m/z* (421.759, 1,106.056, 737.707 and 523.286) were excluded from the fragmentation.

Ion-spray voltage was 2.3–2.4 kV, and nitrogen was used as curtain- and collision gas. Declustering and focusing potentials were set at 65 and 200 V, respectively. For the TOF scans, ion release time and width of six and 5 µs were used. For MS/MS IDA experiments, collision energy was ramped.

The instrument was calibrated on known monoisotopic peaks of 2^+ and 3^+ charged ions of a tryptic digest of myoglobin or ACTH clip (Sigma–Aldrich).

The spectral processing, peak list generation, and database search from raw data were performed on a separate workstation using Analyst QS v1.1 software (Applied Biosystems) linked with the MASCOT Search v1.6b13 script (http://www.matrixscience.com) for Analyst QS (Perkins et al. 1999). The searches were carried out against the mammalian subset of the NCBInr 20080410 database, which contained 683,298 sequences. Parent ion and fragment mass tolerances were 0.15 and 0.8 Da, respectively. No fixed modifications were considered, but carbamidomethylation and carboxymethylation of cysteines (C), and oxidation of methionine (M) were selected as variable modifications. One missed cleavage site was allowed per spot. With the selected search parameters, only results with statistical significance of *P* values lesser than 0.05 (or significance better than 95%) were considered as hits (indicating identity or extensive homology).

Liver SSAT activity

The hepatic SSAT activities of three animals per genotype were assayed using the method of Bernacki (1995).

Liver ATP levels

ATP levels of five animals per mouse line were measured. The liver pieces were homogenized in 5% perchloric acid. The soluble part of the homogenate was neutralized with 3.75 M potassium carbonate. ATP was quantified using the ATPlite 1step kit (Perkin Elmer, Waltham, MA, USA).

Liver nucleoside levels

Tissue levels of nucleosides *S*-adenosyl-L-methionine (AdoMet) and *S*-adenosylhomocysteine (AdoHcy) of five animals per line were determined by HPLC as previously described (She et al. 1994).

Liver catalase activity

Catalase activity was measured from four animals per genotype. The catalase activity was measured as the decrease of absorbance at 240 nm as previously published (Merentie et al. 2007).

Liver glutathione *S*-transferase (GST) activity

The total GST activity was assayed using the method of Habig and Jakoby (1981). The determination is based on the reaction of glutathione with 1-chloro-2,4-dinitrobenzene (CDNB). The reactions were performed in 1 mL quartz cuvettes. Each cuvette contained 980 µL of phosphate-buffered saline, 10 µL of 200 mM reduced glutathione, and 10 µL 100 mM CDNB. Five microliters of a 1:100 dilution of sample extract was included in the reaction mixture and the absorbance at 340 nm was recorded every 30 s for 5 min.

Immunoblotting

A tissue sample of about 100 mg was homogenized with the help of a mechanical potter homogenizer in RIPA buffer containing 50 mM Tris-HCl pH 7.4, 150 mM NaCl, 1 mM EDTA, 1% Triton X-100, 0.5% Na-deoxycholate, 0.1% SDS, 10% glycerol, 1 mM Na_3VO_4, and complete protease inhibitor cocktail (Roche). The protein concentration of the soluble fraction was determined using the Bradford protein assay (Bio-Rad). A total of 20 μg of protein was loaded per sample on 8 or 12% SDS–PAGE gels. Proteins were transferred onto Immobilon FL membranes (Millipore, Billerica, MA, USA). The membranes were probed against PGC-1α (Chemicon, Temecula, CA, USA) and β-actin (Santa Cruz Biotechnology). Horseradish peroxidase-labeled secondary antibodies in conjunction with the ECL plus substrate (GE Healthcare) were used for the protein detection. The membranes were scanned using a Typhoon Variable Mode Imager (GE Healthcare), and the appropriate bands quantified with the ImageQuantTL v.7.0 software (GE Healthcare). Protein expression values were normalized to β-actin levels.

RT–PCR

Total liver RNA of 8 month-old mice was isolated using the Qiazol reagent according to manufacturer's protocol (Qiagen, Germany). The RNA was treated with DNase I (Promega) prior to cDNA synthesis, with the use of a high-capacity cDNA archive kit (Applied Biosystems, Foster City, CA). The RT–PCR running conditions were 2 min at 50°C, 10 min at 95°C, and 40 cycles of 15 s at 95°C and 1 min at 60°C. The primers and probes were designed using an assay by design software (Applied Biosystems). The data were normalized to β-actin expression. Primers sequences are available from the author upon request.

Plasma glucose and insulin levels

Samples were obtained from un-anesthetized mice fasted for 12 h. Blood samples were collected from the tail vein. Plasma glucose values were measured fluorometrically (Passonneau and Lowry 1993). Plasma insulin was measured using a rat insulin enzyme-linked immunosorbent assay (ELISA) (Crystal Chem Inc., Chicago, IL, USA) using mouse insulin as a standard.

Statistical analysis

The results were statistically analyzed using Student's *t*-test. The SPSS v14.0 software package (SPSS) was used for the statistical analysis. The results are expressed as mean ± SEM.

Results

2D-PAGE analysis

A total of 23 spots were found to be differentially expressed between the transgenic and the non-transgenic lines (Fig. 1), 21 of which were positively identified by MS (Table 1). Overall, when compared with the non-transgenic mice, 13 of the identified proteins were repressed, seven were overexpressed, and one spot was not present. As expected, a substantial portion of the identified proteins were found to be directly related to polyamine metabolism (Fig. 2): the expression of fumarate hydratase (spot 10) was elevated by twofold, and that of methionine adenosyltransferase 1 (spot 11) by 1.6-fold. Proteins related to the xenobiotic metabolism were also found to be widely represented: carbonic anhydrase III (spots 6 and 7), repressed by 85 and 60%; selenium-binding protein 2 (spots 14 and 15), repressed by 83 and 67%; 60-kDa heat-shock protein (spot 17), elevated by 2.5-fold; epoxide hydrolase (spot 18), repressed by 58%. The third group combined the proteins which function in the polyamine and xenobiotic metabolisms: glutathione *S*-transferase pi (GST pi) (spots 3 and 4), repressed by 68 and 66%; aldehyde dehydrogenase (spot 12), elevated by 2.5-fold; and catalase (spot 19), repressed by 57%. The last group combined the rest of proteins: major urinary protein 3 (spot 1), repressed by 84%; ferritin light chain subunit 1 (spot 2), elevated by twofold; UTP-glucose 1 phosphate uridylyltransferase 2 (spot 13), repressed by 55%; formimidoyltransferase-

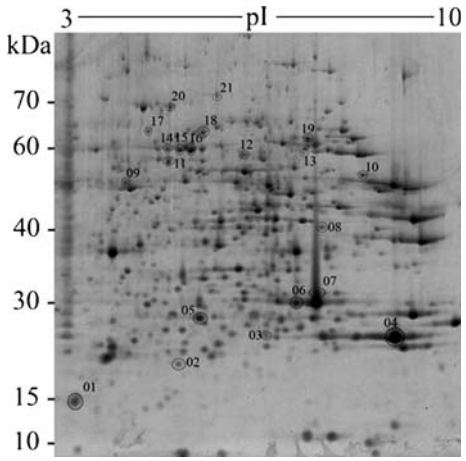

Fig. 1 2D-PAGE of proteins of a non-transgenic mouse liver after SYPRO Ruby stain. Each *numbered circle* shows one of the differentially expressed proteins. 150 μg of liver protein extracts was run in an IPG gel with the pI range 3–10 shown on the *top* of the figure. The second dimension was run using 12.5% polyacrylamide gels that were stained with SYPRO Ruby. The approximate molecular mass (kDa) is shown on the *left side* of the figure

Table 1 List of proteins differentially expressed in the livers of MT-SSAT transgenic versus non-transgenic mice

Spot	Protein	Mr	pI	Fold change	gI	EC
Polyamine metabolism-related proteins						
08	Proteasome 26S subunit, ATPase 6	44,199	6.8	2.5**	28175479	
10	Fumarate hydratase	54,336	9.12	2.0**	33859554	4.2.1.2
11	Methionine adenosyltransferase 1	43,481	5.51	1.6*	19526790	2.5.1.6
Xenobiotic metabolism-related proteins						
06	Carbonic anhydrase III	29,383	6.89	0.15***	31982861	4.2.1.1
07	Carbonic anhydrase III	29,383	6.89	0 4**	31982861	4.2.1.1
14	Selenium-binding protein 2	52,594	5.78	0 17***	9507079	
15	Selenium-binding protein 2	52,594	5.78	0.33*	9507079	
17	Heat-shock protein 60	60,903	5.91	2.5**	51455	
18	Epoxide hydrolase	62,503	5.96	0.42**	74218511	3.3.2.10
Polyamine and xenobiotic metabolisms-related proteins						
03	Glutathione *S*-transferase pi	23,463	8.13	0.32*	576133	2.5.1.18
04	Glutathione *S*-transferase pi	23,463	8.13	0.34*	576133	2.5.1.18
05	Indolethylamine *N*-methyltransferase	29,441	6	NP	6678281	2.1.1.49
12	Aldehyde dehydrogenase	56,502	7.53	2.5**	6753036	1.2.1.3
19	Catalase	59,728	7.72	0.43**	115704	1.11.1.6
Other proteins						
01	Major urinary protein 3	20,650	5.04	0.16***	127527	
02	Ferritin light chain subunit 1	20,790	5.66	2.0*	120524	
09	Actin	39,161	5.78	0 42***	49868	
13	UTP-glucose-1-phosphate uridylyltransferase 2	56,944	7.18	0.45**	21314832	2.7.7.9
16	Formimidoyltransferase-cyclodeaminase	58,902	5.79	0.71*	18252784	2.1.2.5 4.3.1.4
20	Albumin	68,678	5.75	3.3**	26340966	
21	Histidine ammonia lyase	72,212	5.94	0.53*	6754152	4.3.1.3

Spot number corresponds to the numbering used in Fig. 1; Mr and pI are the theoretical values for each protein retrieved from the Uniprot database (http://www.uniprot.org); Fold change <1 repressed or >1 overexpressed versus the non-transgenic mice, and significance value $*P < 0.05$, $** P < 0.01$ or $***P < 0.001$, *NP* not present, *gI* is the access code from the Entrez Protein database (http://www.ncbi.nlm.nih.gov/protein); EC lists the enzyme commission number for each one of the enzymes

cyclodeaminase (spot 16), repressed by 29%; albumin (spot 20), elevated by 3.3-fold; and histidine ammonia lyase (spot 21), repressed by 47%.

Enzyme activities of polyamine metabolism enzyme, nucleosides levels, and hepatic ATP content

Hepatic SSAT activity in MT-SSAT transgenic mice was increased 34-fold without induction (Fig. 3a). Enhanced polyamine catabolism is directly linked to activated polyamine biosynthesis, which demonstrated by the activation of the two rate-controlling enzymes. We showed earlier that hepatic ornithine decarboxylase (ODC, EC 4.1.1.17) was increased more than 100-fold, and that of *S*-adenosyl-L-methionine decarboxylase (AdoMetDC, EC 4.1.1.5) by twofold when compared with the non-transgenic mice (Suppola et al. 1999). Moreover, the activation of polyamine biosynthesis was associated with 54% depletion the level of AdoMet, whereas the level of AdoHcy remained unchanged in the liver of transgenic mice (Fig. 3b). Hepatic ATP content was reduced by 59% in the transgenic mice in comparison with the non-transgenic mice (Fig. 3c).

Catalase and GST activities

The expression of the two enzymes that were found repressed in the 2D-PAGE analysis was examined further. Catalase expression was reduced by 57% in the transgenic mice (Table 1), and its catalytic activity was reduced accordingly by 65% ($P < 0.05$) (Fig. 4a). The second enzyme analyzed further was GST pi, the expression of which was reduced by 68 and 66% in the transgenic mice (Table 1). The total GST activity was reduced to 80% in the transgenic line when compared with the non-transgenic mice ($P < 0.05$) (Fig. 4b).

Hepatic PGC-1α protein expression, gluconeogenic gene expression, and plasma glucose and insulin levels

Western blot analysis revealed that the expression of PGC-1α protein was increased by 3.5-fold in the MT-SSAT

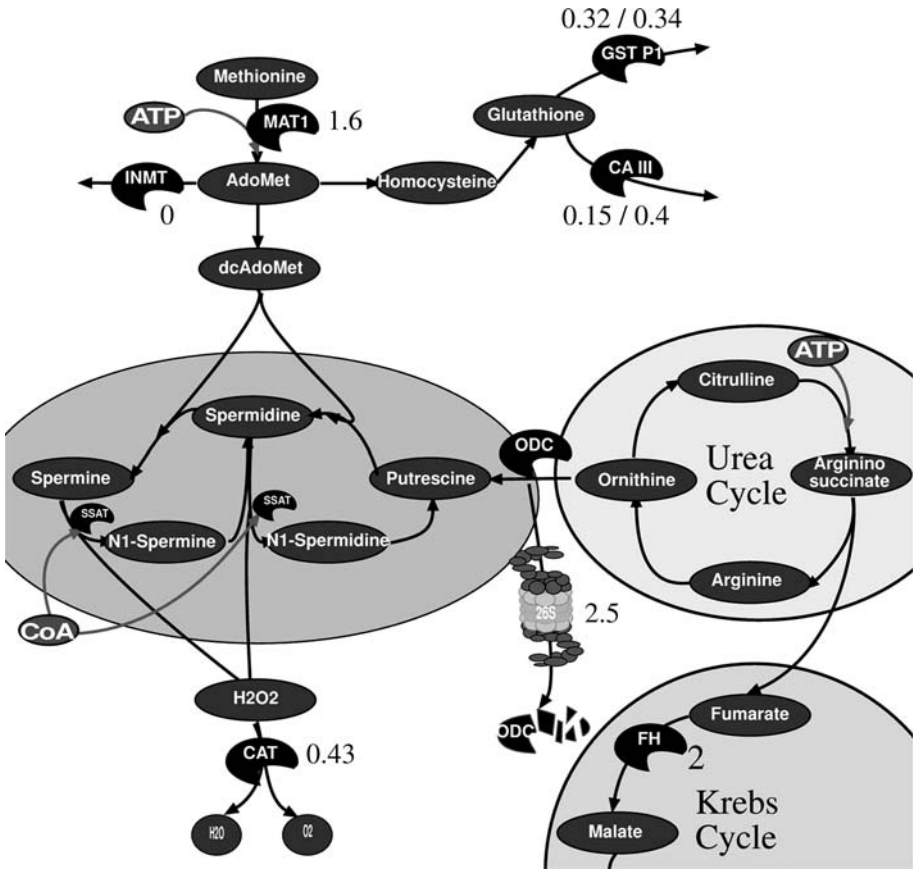

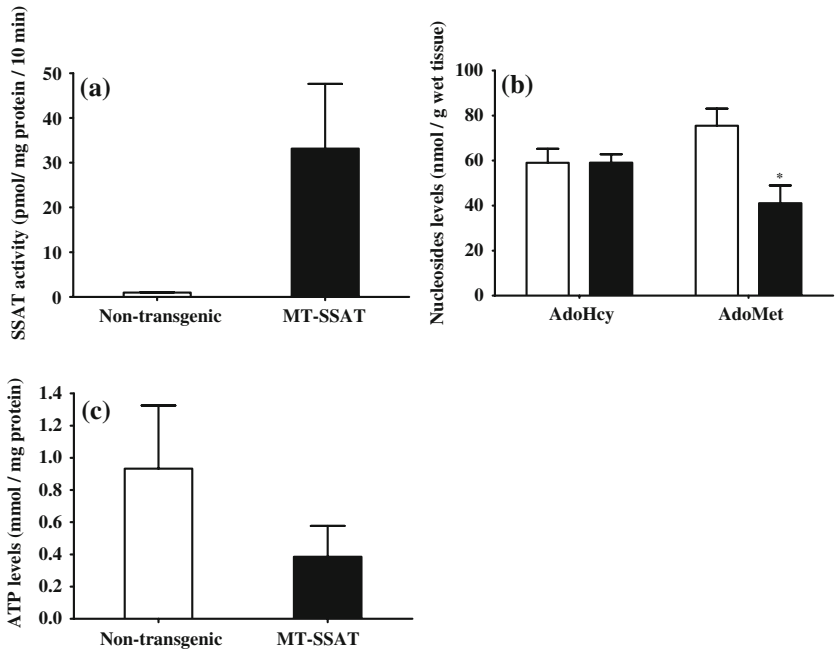

Fig. 2 Metabolic overview of the polyamine cycle and related pathways. The levels of expression of the differently expressed proteins are marked as *numbers* showing the fold difference in transgenic mice in comparison with the non-transgenic mice

Fig. 3 SSAT activities, nucleoside levels, and hepatic ATP levels. **a** Liver SSAT activity (nmol/μg protein/10 min) is expressed as mean ± SEM obtained from three non-transgenic or transgenic mice. **b** Nucleoside levels (μmol/μg wet tissue) were measured by HPLC and are expressed as mean ± SEM from five non-transgenic and four transgenic animals. *$P = 0.05$. **c** Liver ATP level (μmol/μg protein) is expressed as mean ± SEM obtained from eight animals per genotype. *White bars* represent the non-transgenic mice and the *black bars* represent the transgenic mice

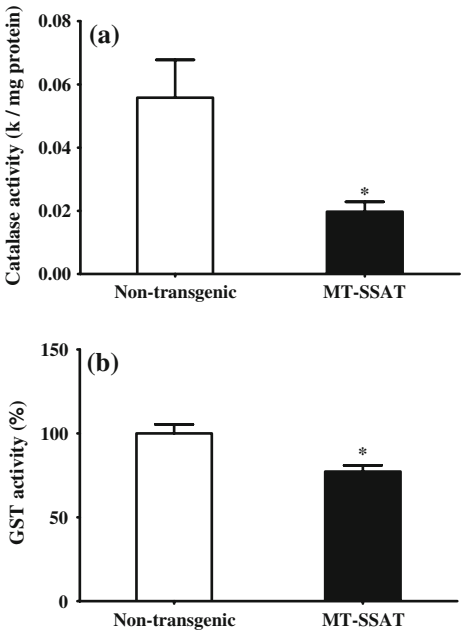

Fig. 4 Liver catalase and glutathione *S*-transferase activities. **a** Liver catalase activities (K/μg protein) were measured by the method of Aebi. Data are expressed as mean ± SEM obtained from four animals per genotype; $*P < 0.05$. **b** The method from Habig and Jakoby was used to measure the hepatic GST activity. Data are expressed as percentage (%) of the value for non-transgenic mice (mean ± SEM). Data were obtained from five non-transgenic and four transgenic animals; $*P < 0.05$

transgenic mice when compared with their non-transgenic littermates ($P < 0.001$) (Fig. 5a). Moreover, we also measured using RT–PCR the expression levels of key gluconeogenic genes that are under the control of PGC-1α. The expression levels of phosphoenolpyruvate carboxykinase (Pepck) and glucose-6-phosphatase (G6PC-1) were found to be elevated 3.5- and 4-fold, respectively, in the transgenic mice (Fig. 5b). MT-SSAT transgenic mice showed 45 and 18% decrease in the basal plasma insulin and glucose levels, respectively, when compared with the non-transgenic mice (Fig. 5c).

Discussion

Ubiquitous overexpression of the rate-limiting enzyme of the polyamine catabolism in separate transgenic mouse lines leads to a particular phenotype regardless of the promoter used in the transgene construct (Pietilä et al. 1997; Suppola et al. 1999). Both transgenic mouse lines (SSAT and MT-SSAT) are characterized by increased tissue putrescine level and decreased levels of spermidine and spermine. Moreover, the transgenic mice become hairless between the 8 and 14 weeks of age, and their skin appears extremely wrinkled (Suppola et al. 1999). Even though the metallothionein I promoter targets SSAT transgene to liver and pancreas, SSAT activation in the rest of organs was

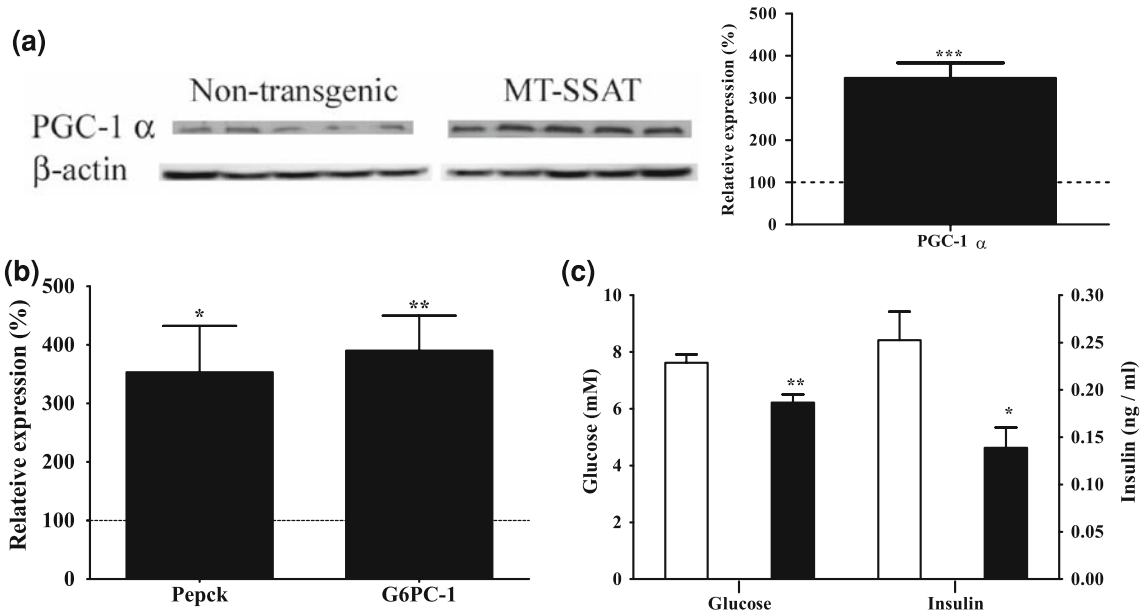

Fig. 5 Hepatic PGC-1α protein levels, gluconeogenic gene expression, and plasma glucose and insulin levels. **a** Liver PGC-1α protein levels are normalized against expression levels of *β*-actin. The data (mean ± SEM) are expressed as percentage (%) of the value for non-transgenic mice. Data were obtained from five mice per genotype. $***P < 0.001$. **b** Liver Pepck and G6PC-1 mRNA expression levels from five animals per genotype. The data (mean ± SEM) are expressed as percentage (%) of the value for non-transgenic mice after normalization to 18S RNA. Data were obtained from five animals per genotype. $*P < 0.05$, and $**P < 0.01$. **c** Plasma glucose (mM) and insulin (ng/ml) levels in non-transgenic (*white bars*) and transgenic (*black bars*) mice. The data are expressed as mean ± SEM obtained from eight animals per genotype. $*P < 0.05$ and $**P < 0.01$

also seen. We performed 2D-PAGE analysis to study at the protein level on how the SSAT activation and subsequent changes in the polyamine metabolism affect the liver protein expression in the MT-SSAT mouse line.

In SSAT transgenic mice, the activation of the polyamine catabolism is accompanied with compensatory elevated polyamine biosynthesis to maintain the cellular polyamine levels. The two rate-controlling enzymes of the polyamine biosynthesis, namely ODC and AdoMetDC show 100- and 2-fold higher activities, respectively, in the MT-SSAT transgenic mice in comparison with non-transgenic littermates (Suppola et al. 1999). Signs of the enhanced biosynthesis were also seen during the 2D-PAGE analysis, as methionine adenosyltransferase, the enzyme that catalyzes the conversion of methionine to AdoMet (Fig. 2), was found to be overexpressed by 1.6-fold in the transgenic mice. Consistently, transgenic animals showed 50% lower levels of AdoMet, in agreement with the enhanced production of decarboxylated *S*-adenosyl-L-methionine (dcAdoMet) by the action of AdoMetDC (Fig. 3b).

Polyamine catabolism produces hydrogen peroxide and 3-acetamidopropanal as toxic by-products. Hydrogen peroxide is toxic by itself, and 3-aminopropanal is spontaneously converted to the toxic product acrolein by β-elimination (Seiler 2004). In animals overexpressing SSAT, increased polyamine catabolism would create elevated amounts of the two by-products. The by-products would need to be detoxified to avoid harmful consequences in the tissue. Indeed, 2D-PAGE showed that aldehyde dehydrogenase, an enzyme necessary for the detoxification of 3-aminopropanal, was elevated 2.5-fold in transgenic mice. Surprisingly, the expression of catalase, needed for the detoxification of hydrogen peroxide, was reduced to 43%, and its hepatic activity was decreased to 35% (Fig. 4a).

The hepatic ATP level was decreased by 59% in the transgenic mice when compared with non-transgenic mice (Fig. 3c). The low ATP levels could be due to the energy consumed during polyamine metabolism. A complete turn on the polyamine cycle consumes five ATP equivalents, two of them during the formation of AdoMet from methionine, two for the production of cytosolic acetyl-CoA, and the last one consumed in the novo synthesis of putrescine during the conversion of citrulline to argininosuccinate, the arginine precursor in the urea cycle (Jänne et al. 2005) (Fig. 2). We showed earlier that the co-activator PGC-1α is overexpressed in the WAT of the SSAT transgenic mice, most likely in response to depletion of ATP pools (Pirinen et al. 2007). Here, we assayed the PGC-1α expression in the livers of MT-SSAT mice. Western blotting analysis revealed that the transgenic mice had 3.5 times higher expression of PGC-1α than their non-transgenic littermates (Fig. 5a). PGC-1α is also one of the main controllers of the liver gluconeogenic program (Rodgers et al. 2005). Therefore, we then further investigated the expression level of key gluconeogenic genes, Pepck and G6PC-1, and found that they were increased by 3.5- and 4-fold, respectively, in the transgenic livers in fed state (Fig. 5b). We cannot definitely distinguish whether the lower ATP levels come from the polyamine catabolism activation, or from enhanced gluconeogenesis, or from a combination of both. Nonetheless, such low ATP levels would most likely trigger specific mechanisms aimed in protecting the cells from a possible energy shortage. It has previously been reported that the activation of the 60-kDa heat-shock protein helps to recover the ATP levels in rat cardiac myocytes following ischemic injury (Lin et al. 2001). It was interesting to note that according to 2D-PAGE analysis, this protein was overexpressed by 2.5-fold in the transgenic livers.

Another protein found overexpressed in the transgenic mice was ferritin, which was elevated by twofold. Ferritin is composed of 24 different subunits and functions as the main iron storage molecule in the cell. Ferritin works as an iron donor in the heme production, where an iron atom is attached in the middle of a porphyrin ring (Mazur and Carleton 1963). A recent work reported that PGC-1α positively regulates the rate-limiting enzyme in the hepatic heme biosynthesis (Handschin et al. 2005) indicating that PGC-1α may also be the mediator of ferritin overexpression in our transgenic mice. Moreover, decreased expression levels of GST pi and selenium-binding protein 2, similar to those revealed by 2D-PAGE in the MT-SSAT transgenic mice, have been associated with elevated expression of peroxisome proliferator-activated receptor α (Chu et al. 2004; Giometti et al. 2000) a known target of PGC-1α (Finck and Kelly 2006).

Activation of hepatic PGC-1α is considered as a sign of diabetes due to its control over the gluconeogenesis that might increase hepatic glucose output (Koo et al. 2004). Therefore, the possibility that the MT-SSAT mice would show impaired insulin sensitivity prompted us to analyze the fasting plasma glucose and insulin levels. In contrast to the expected, the transgenic animals showed fasting hypoglycemia (20% lower than in control mice; $P < 0.01$) and hypoinsulinemia (45% lower than in control mice; $P < 0.05$) (Fig. 5c). In all likelihood, PGC-1α activation is directly linked to the activation of polyamine catabolism in the tissues of transgenic mice. We have previously shown that elevated PGC-1α is seen in the WAT of SSAT transgenic mice (Pirinen et al. 2007). In MT-SSAT mice, PGC-1α may also be activated in the rest of tissues, especially in the WAT and muscle, thus potentially increasing their insulin sensitivity. Activation of PGC-1α has also been shown after resveratrol treatment. Resveratrol is a polyphenolic compound of plant origin, with the ability to increase lifespan and improve insulin sensitivity through the activation of Sirt 1, which de-acetylates and activates

PGC-1α (Lagouge et al. 2006). Resveratrol-treated mice increase the expression and activity of PGC-1α in the WAT, muscle and liver, and the animals become insulin sensitive, despite the increased gluconeogenesis (Baur et al. 2006). In the MT-SSAT transgenic line, the hepatic Sirt 1 protein levels were not changed (data not shown), indicating that the control of PGC-1α in these animals may go through a different mechanism than after resveratrol treatment, possibly involving polyamines themselves. Therefore, we suggest that general activation of PGC-1α, similar to that obtained with the resveratrol treatment, causes insulin sensitivity in animals with accelerated polyamine catabolism. We further found that major urinary protein 3 (MUP3), which belongs to the lipocalin family, was greatly downregulated in the transgenic mice. Another member of the lipocalin family is the retinol-binding protein 4. This protein has gained much attention lately due to its positive correlation with insulin resistance (Yang et al. 2005). We may speculate that MUP3, just as retinol-binding protein 4, may also be predictive of increased insulin sensitivity.

To conclude, our results indicate that the changes seen in the hepatic proteomic pattern of the transgenic animals result directly from activated polyamine catabolism. The expression pattern of some proteins is apparently attributable to the hepatic activation of PGC-1α. PGC-1α is also likely activated in other tissues of the transgenic mice producing improved insulin sensitivity and glucose tolerance, similarly as with resveratrol treatment. This mechanism has proven to work in other animal models, as well as with humans. It is exciting to see whether new treatment approaches for insulin resistance could involve the use of polyamine analogs capable of activating polyamine catabolism.

Acknowledgments This work was supported by the Academy of Finland.

References

Baur JA, Pearson KJ, Price NL et al (2006) Resveratrol improves health and survival of mice on a high-calorie diet. Nature 444:337–342

Bernacki RJ, Oberman EJ, Seweryniak KE, Atwood A, Bergeron RJ, Porter CW (1995) Preclinical antitumor efficacy of the polyamine analogue N^1, N^{11}-diethylnorspermine administered by multiple injection or continuous infusion. Clin Cancer Res 1:847–857

Chu R, Lim H, Brumfield L, Liu H, Herring C, Ulintz P, Reddy JK, Davison M (2004) Protein profiling of mouse livers with peroxisome proliferator-activated receptor alpha activation. Mol Cell Biol 24:6288–6297

Finck BN, Kelly DP (2006) PGC-1 coactivators: inducible regulators of energy metabolism in health and disease. J Clin Invest 116:615–622

Giometti CS, Liang X, Tollaksen SL, Wall DB, Lubman DM, Subbarao V, Rao MS (2000) Mouse liver selenium-binding protein decreased in abundance by peroxisome proliferators. Electrophoresis 21:2162–2169

Görg A, Obermaier C, Boguth G, Harder A, Scheibe B, Wildgruber R, Weiss W (2000) The current state of two-dimensional electrophoresis with immobilized pH gradients. Electrophoresis 21:1037–1053

Habig WH, Jakoby WB (1981) Glutathione *S*-transferases (rat and human). Methods Enzymol 77:218–231

Handschin C, Lin J, Rhee J, Peyer AK, Chin S, Wu PH, Meyer UA, Spiegelman BM (2005) Nutritional regulation of hepatic heme biosynthesis and porphyria through PGC-1alpha. Cell 122:505–515

Jänne J, Alhonen L, Pietilä M, Keinänen TA (2004) Genetic approaches to the cellular functions of polyamines in mammals. Eur J Biochem 271:877–894

Jänne J, Alhonen L, Keinänen TA, Pietilä M, Uimari A, Pirinen E, Hyvönen MT, Järvinen A (2005) Animal disease models generated by genetic engineering of polyamine metabolism. J Cell Mol Med 9:865–882

Järvinen AJ, Cerrada-Gimenez M, Grigorenko NA, Khomutov AR, Vepsäläinen JJ, Sinervirta RM, Keinänen TA, Alhonen LI, Jänne JE (2006) Alpha-methyl polyamines: efficient synthesis and tolerance studies in vivo and in vitro. First evidence for dormant stereo specificity of polyamine oxidase. J Med Chem 49:399–406

Koo S, Satoh H, Herzig S, Lee CH, Hedrick S, Kulkarni R, Evans RM, Olefsky J, Montminy M (2004) PGC-1 promotes insulin resistance in liver through PPAR-alpha-dependent induction of TRB-3. Nat Med 10:530–534

Lagouge M, Argmann C, Gerhart-Hines Z et al (2006) Resveratrol improves mitochondrial function and protects against metabolic disease by activating SIRT1 and PGC-1alpha. Cell 127:1109–1122

Lin KM, Lin B, Lian IY, Mestril R, Scheffler IE, Dillmann WH (2001) Combined and individual mitochondrial HSP60 and HSP10 expression in cardiac myocytes protects mitochondrial function and prevents apoptotic cell deaths induced by simulated ischemia-reoxygenation. Circulation 103:1787–1792

Mann M, Wilm M (1994) Error-tolerant identification of peptides in sequence databases by peptide sequence tags. Anal Chem 66:4390–4399

Mazur A, Carleton A (1963) Relation of ferritin iron to heme synthesis in marrow and reticulocytes. J Biol Chem 238:1817–1824

Merentie M, Uimari A, Pietilä M, Sinervirta R, Keinänen TA, Vepsäläinen J, Khomutov A, Grigorenko N, Herzik KH, Jänne J, Alhonen L (2007) Oxidative stress and inflammation in the pathogenesis of activated polyamine catabolism-induced acute pancreatitis. Amino Acids 33:323–330

Niiranen K, Keinänen TA, Pirinen E, Heikkinen S, Tusa M, Fatrai S, Suppola S, Pietilä M, Uimari A, Laakso M, Alhonen L, Jänne J (2006) Mice with targeted disruption of spermidine/spermine N^1-acetyltransferase gene maintain nearly normal tissue polyamine homeostasis but show signs of insulin resistance upon aging. J Cell Mol Med 10:933–945

Park MH, Lee YB, Joe YA (1997) Hypusine is essential for eukaryotic cell proliferation. Biol Signals 6:115–123

Passonneau JV, Lowry OH (1993) Enzymatic analysis: a practical guide. Humana Press, New Jersey. doi:10.1226/0896032388

Perkins DN, Pappin DJ, Creasy DM, Cottrell JS (1999) Probability-based protein identification by searching sequence databases using mass spectrometry data. Electrophoresis 20:3551–3567

Pietilä M, Alhonen L, Halmekytö M, Kanter P, Jänne J, Porter CW (1997) Activation of polyamine catabolism profoundly alters tissue polyamine pools and affects hair growth and female

fertility in transgenic mice overexpressing spermidine/spermine N^1-acetyltransferase. J Biol Chem 272:18746–18751

Pirinen E, Kuulasmaa T, Pietilä M et al (2007) Enhanced polyamine catabolism alters homeostatic control of white adipose tissue mass, energy expenditure, and glucose metabolism. Mol Cell Biol 27:4953–4967

Rodgers JT, Lerin C, Haas W, Gygi SP, Spiegelman BM, Puigserver P (2005) Nutrient control of glucose homeostasis through a complex of PGC-1alpha and SIRT1. Nature 434:113–118

Seiler N (2004) Catabolism of polyamines. Amino Acids 26:217–233

She QB, Nagao I, Hayakawa T, Tsuge H (1994) A simple HPLC method for the determination of S-adenosylmethionine and S-adenosylhomocysteine in rat tissues: the effect of vitamin B6 deficiency on these concentrations in rat liver. Biochem Biophys Res Commun 205:1748–1754

Suppola S, Pietilä M, Parkkinen JJ, Korhonen VP, Alhonen L, Halmekytö M, Porter CW, Jänne J (1999) Overexpression of spermidine/spermine N^1-acetyltransferase under the control of mouse metallothionein I promoter in transgenic mice: evidence for a striking post-transcriptional regulation of transgene expression by a polyamine analogue. Biochem J 338:311–316

Wallace HM, Fraser AV (2004) Inhibitors of polyamine metabolism: review article. Amino Acids 26:353–365

Wallace HM, Fraser AV, Hughes A (2003) A perspective of polyamine metabolism. Biochem J 376:1–14

Yang Q, Graham TE, Mody N, Preitner F, Peroni OD, Zabolotny JM, Kotani K, Quadro L, Kahn BB (2005) Serum retinol binding protein 4 contributes to insulin resistance in obesity and type 2 diabetes. Nature 436:356–362